J Appl Electrochem (2012) 42:375–381
DOI 10.1007/s10800-012-0407-3

ORIGINAL PAPER

Electrodeposit nano-copper oxide on glassy carbon electrode for simultaneous detection of guanine and adenine

Xiaoyan Zhang · Xian Liang · Mai Xu · Xia Bao · Fengwu Wang · Zhousheng Yang

Received: 7 February 2012 / Accepted: 21 March 2012 / Published online: 3 April 2012

Abstract An electrochemical sensor was fabricated and used to simultaneously detect guanine and adenine. In this study, nano-copper oxide-modified glassy carbon electrode (nano-copper oxide/GCE) was prepared by electrodeposition. The nano-copper oxide/GCE was characterized by electrochemical impedance spectroscopy and scanning electron microscopy. The fabricated nano-copper oxide/GCE sensor exhibited sensitive response to guanine and adenine in 0.1 M PBS (pH 7.0). The anodic peak currents were linear with the guanine and adenine concentrations over the range of 0.05–1.2 μM with the correlation coefficients of 0.9997 and 0.9993, respectively, and the corresponding detection limits were 6×10^{-3} μM and 9×10^{-3} μM (S/N = 3), respectively. The nano-copper oxide/GCE could be applied to simultaneously detect guanine and adenine in samples with good anti-interference ability.

Keywords Nano-copper oxide · Glassy carbon electrode · Electrodeposition · Guanine · Adenine · Simultaneous detection

1 Introduction

Nucleic acids offer the analytic chemist a powerful tool for the recognition and monitoring of many important compounds [1]. Oxidative stress initiates DNA modification and mutagenic lesions that contribute to pathologic processes in various diseases, including cancer [2, 3]. The bases (purines and pyrimidine) present in DNA form hydrogen bonds between them with their respective complementary base, which plays a vital role in biologic systems [4]. The abnormal changes of the bases in organism suggest the deficiency and mutation of the immunity system, indicating the presence of various diseases. Guanine and adenine are two principal bases found in nucleic acids, playing important roles in many biologic processes. They have widespread effects on coronary and cerebral circulation, control of blood flow, prevention of cardiac arrhythmias, inhibition of neurotransmitter release, and modulation of adenylate cyclase activity [5, 6]. Their concentrations are considered as important parameter for diagnosis of cancers, AIDS, myocardial cellular energy status, disease progress, and therapy responses [7]. Hence, the analysis of these bases has great significance to the bioscience and clinical diagnosis [8].

In recent years, a series of methods, such as micellar electrokinetic chromatography (MEKC), followed by indirect laser-induced fluorescence detection (ILIFD) [9]; HPLC and capillary electrophoresis (CE), followed by UV [10–14]; ion-pairing liquid chromatography (IPLC) [15]; flow injection-chemiluminescence (CL) [16]; and spectroscopic methods, were developed for the detection of guanine and adenine [17, 18]. These methods have gained interest from the researchers in life sciences due to their high efficiency and small sample size requirement, but they need complicated instruments and time-consuming sample pretreatment. The electrochemical method also was applied to investigate electrochemical properties of guanine and adenine. Tang attempted the detection of adenine and guanine at MWCNT-PNF films [19]. Carbon ionic liquid electrode was prepared,

X. Zhang · X. Liang (✉) · M. Xu · X. Bao · F. Wang
Department of Chemistry and Chemical Engineering, Huainan Normal University, Huainan 232001, Anhui, People's Republic of China
e-mail: liangxian226@163.com

Z. Yang
College of Chemistry and Materials Science, Anhui Key Laboratory of Chemo-Biosensing, Anhui Normal University, Wuhu 241000, People's Republic of China

offering a strategy for the simultaneous detection of guanine and adenine [20]. Liu used the polythionine/NPAu/MWNT-modified electrode to determinate the guanine and adenine in DNA [21]. However, the electrode preparation of these methods was complex, and so we should explore a simple method to prepare the electrode for guanine and adenine detection.

Nano-copper oxide, as a well-known p-type semiconductor, has gained increasing attention because of its distinctive properties. The virtues of nano-copper oxides, such as natural abundance, low production cost, high stability, and good electrical properties, make it suitable for the applications in gas sensors, photocatalysts, and electrochemical sensors [22–24]. Liu prepared an electrochemical sensor by electrodepositing nano-copper oxide on glassy carbon electrode (GCE) for H_2O_2 detection [25]. The copper oxide nanowire film was facilely attached to a GCE, and the CuO nanowire electrode showed excellent electrocatalytic response to H_2O_2 [26]. CuO nanospheres were applied to modify the GCE for sensitive nonenzymatic glucose detection [27].

In this study, we prepared nano-copper oxide-modified glassy carbon electrode (nano-copper oxide/GCE) by electrodeposition process. The nano-copper oxide/GCE could improve the oxidation properties of guanine and adenine. The oxidation peak currents of guanine and adenine could be greatly enhanced on nano-copper oxide/GCE. This sensor, prepared using a simple fabrication process, showed an excellent amperometric response to guanine and adenine besides high sensitivity and fast response time, and so it was successfully applied to simultaneously detect guanine and adenine in the samples.

2 Experimental

2.1 Reagents and apparatus

Guanine, adenine, and calf thymus double-stranded DNA (CT-DNA) from Sigma were used without further purification. Stock solutions of CT-DNA, guanine, and adenine were prepared in distilled water and stored at 4 °C. The DNA solution was used within 5 days. All the other chemicals were of analytic grade. Double-distilled water was utilized in all the solutions. The experiments were carried out at room temperature.

All voltammetric measurements were performed using the CHI660A electrochemical analyzer (CHI Instruments, Chenhua Corp., Shanghai, China). The three-electrode system was used in this study. The two working electrodes were bare GCE ($\Phi = 3$ mm) and nano-copper oxide/GCE, respectively. The reference electrode was an Ag/AgCl (saturated KCl) electrode, and platinum electrode was used as the auxiliary electrode. Before each experiment, solutions were purged with high-purity N_2 for 15 min to remove oxygen.

2.2 Modified electrode preparation

The GCE surface was polished to appear mirror-like with fine emery papers and with 0.050 μm alumina slurry and was rinsed with distilled water thoroughly. The water on electrode was dried with high-purity N_2. The copper film was first electrodeposited on GCE surface by maintaining potential of −0.4 V for 200 s in 0.1 mol L^{-1} KCl solution containing 20 μmol L^{-1} $CuCl_2$. Then, the electrode was rinsed with distilled water and dried with N_2. After that, the copper film/GCE was put in 0.1 mol L^{-1} NaOH solution and scanned repetitively for 20 cycles under potentials ranging from −0.5 to 0.3 V at 100 mV s^{-1} to form a nano-copper oxide/GCE [25].

2.3 CT-DNA samples preparation

CT-DNA (2 mg) was digested in 1 ml $HClO_4$ (1 M). The solution was heated by boiling water-bath for an hour, and then pH of the solution was adjusted to 7.0 using 1 M NaOH in boiling state. Finally, the solution was diluted to 5 ml by 0.1 M pH 7.0 PBS to form the denatured CT-DNA solution.

3 Results and discussion

3.1 Characterizations of the modified electrode

The EIS is a powerful tool for studying the interface properties of surface-modified electrodes. The Nyquist plots of impedance spectra include a semicircular portion and a linear portion: the semicircular portion at higher frequencies corresponds to the electron-transfer limited process, and the linear portion at lower frequencies corresponds to the diffusion process. Figure 1a exhibits the Nyquist plots of the GCE (curve a) and nano-copper oxide/GCE (curve b) in 1.0 mM $[Fe(CN)_6]^{3-/4-}$. The Nyquist diameter of the nano-copper oxide/GCE (Rct = 2.8 kΩ) was much larger than that of bare GCE, which indicated that nano-copper oxide was successfully modified on to GCE.

In order to investigate the morphology of nano-copper oxide film, the typical SEM images of nano-copper oxide/GCE were shown in Fig. 1b. It can be seen that a film of nano-copper oxide particles was homogeneously distributed on the surface of GCE. The size of these nano-copper oxide particles was in the range of 50–100 nm, meaning that nano-copper oxide has unusual properties, such as

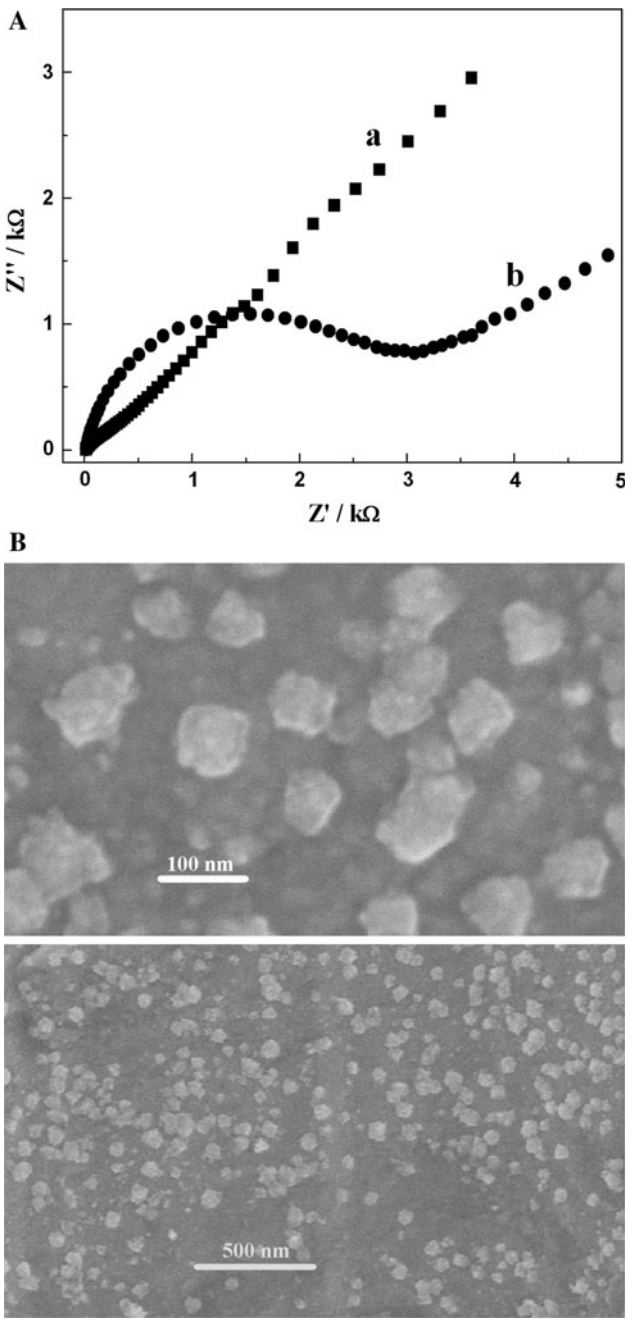

Fig. 1 **a** Nyquist diagrams of 1.0 mM $[Fe(CN)_6]^{3-/4-}$ recorded using bare GCE (*a*) and nano-copper oxide/GCE (*b*). **b** SEM image of nano-copper oxide/GCE surface

large specific surface area and high surface reaction activity, which will help in improving the sensitivity of the nano-copper oxide/GCE.

3.2 Electrochemical behaviors of guanine and adenine at the nano-copper oxide/GCE

The cyclic voltammetric curves of 0.5 μM guanine and 0.5 μM adenine on the GCE, nano-copper oxide/GCE in 0.10 M PBS (pH 7.0) are shown in Fig. 2a. Two oxidation peaks occurred at 0.78 and 1.07 V, no reduction peak yielding in cathode process on cyclic voltammetric curve using the GCE, which indicated that guanine and adenine showed irreversible redox process on GCE. Under the same experimental condition, when using nano-copper oxide/GCE, the oxidation peak current of purine bases was much larger than that on GCE. As the sensitivity of differential pulse voltammetry (DPV) was better than the cyclic voltammetry, the recorded DPV curves of 0.5 μM guanine and 0.5 μM adenine on the GCE and nano-copper oxide/GCE in 0.10 M PBS (pH 7.0) are shown in Fig. 2b. We could also obtain that the oxidation peak currents of guanine and adenine on nano-copper oxide/GCE remarkably enhanced.

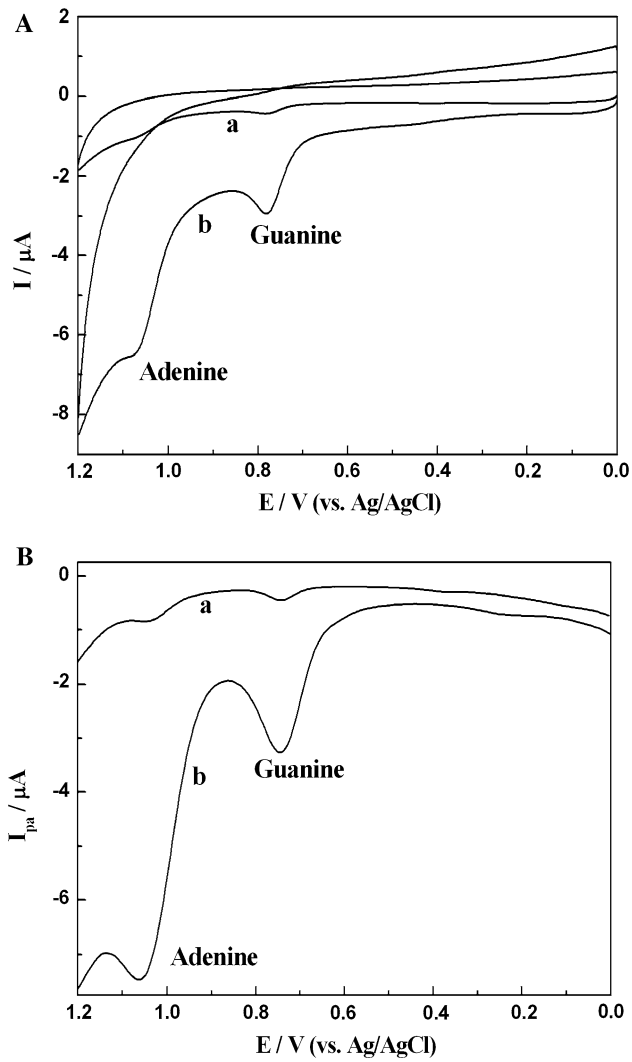

Fig. 2 **a** CV curves of 0.5 μM guanine and 0.5 μM adenine on the bare GCE (*a*) and nano-copper oxide/GCE (*b*) in 0.1 M PBS (pH 7.0). Scan rate: 50 mV s^{-1}. **b** DPV curves of 0.5 μM guanine and 0.5 μM adenine on the bare GCE (*a*) and nano-copper oxide/GCE (*b*) in 0.1 M PBS (pH 7.0)

The dependence of the peak currents of guanine and adenine on nano-copper oxide/GCE on the scan rate is shown in Fig. 3. With the increase of scan rate, the anodic peak currents of guanine and adenine increased linearly with the correlation coefficients being $R = 0.9993$ and $R = 0.9995$, respectively. This result indicated that the oxidation process of guanine and adenine on nano-copper oxide/GCE was controlled by adsorption.

3.3 Factors influencing the behaviors of guanine and adenine on the nano-copper oxide/GCE

The effect of copper film deposition potential for the electrochemical response of purine bases on nano-copper oxide/GCE was examined in 0.1 M PBS at various potential values ranging from −0.2 to −0.7 (Fig. 4a). The anodic peak current improved with decreasing potential value, and reached the maximum value when potential value was equal to −0.4 V. Afterward, the anodic peak current decreased with potential value <−0.4 V. Because the more negative was the deposition potential, the higher was the catalytic activity, indicating that the number of active sites of nano-copper oxide film played a major role. However, the catalytic ability decreased when the deposition potential was lower than −0.4 V, which may be attributed to the increase of resistance of ion transfer for charge balance in the process of film oxidation and reduction [25]. Hence, the optimal deposition potential should be −0.4 V.

Figure 4b showed that the deposition time of nano-copper oxide influenced on oxidation peak current of guanine and adenine. The deposition time determined the copper film thickness and indirectly influenced the nano-copper oxide film thickness on GCE. The nano-copper oxide film could not completely coat the surface of GCE for the deposition time less than 100 s and lead to an insufficient number of active sites. With the deposition time increasing, the morphology of deposited nano-copper oxide may change from particles to film, which could decrease the active sites [25]. So we chose 200 s as the suitable deposition time according to the experiment result.

The influence of the solution pH on the electrochemical response of guanine and adenine on nano-copper oxide/GCE was examined in 0.1 M PBS at various pH values ranging from 3.0 to 9.0. The corresponding results were shown in Fig. 5. It could be seen that the anodic peak potential shifted toward negative values linearly, and linear regression equations $E_{pa} = 1.118 - 0.058$ pH (peak

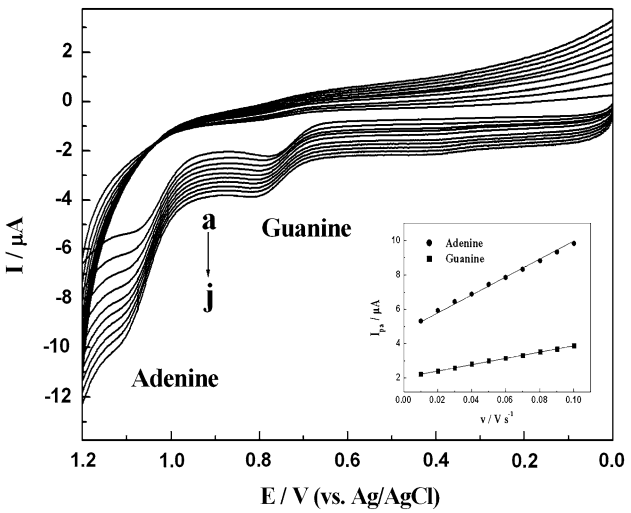

Fig. 3 CV curves of 0.5 μM guanine and 0.5 μM adenine on the nano-copper oxide/GCE at different scan rates in 0.1 M PBS (pH 7.0): (*a*) 10, (*b*) 20, (*c*) 30, (*d*) 40, (*e*) 50, (*f*) 60, (*g*) 70, (*h*) 80, (*i*) 90, and (*j*) 100 (mV s^{-1}). *Inset*: plot of anodic peak current versus scan rate

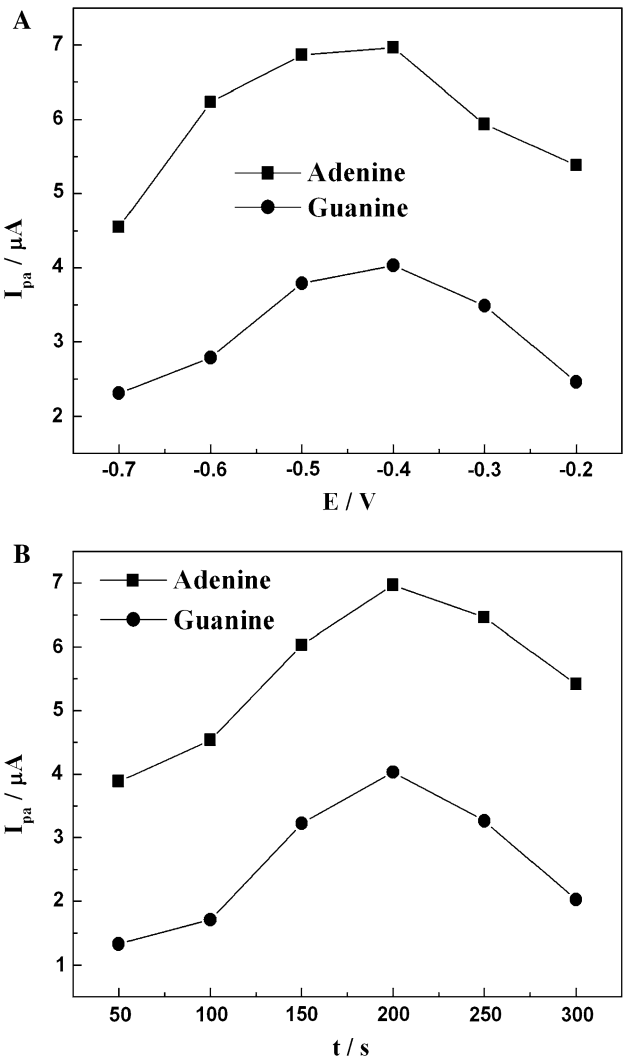

Fig. 4 **a** Effect of deposition potential for nano-copper oxide film formation of nano-copper oxide/GCE. **b** Effect of deposition time for nano-copper oxide film formation of nano-copper oxide/GCE

guanine), $E_{pa} = 1.448-0.061$ pH (peak adenine) could be obtained with the correlation coefficients of 0.9993 (peak guanine) and 0.9992 (peak adenine), respectively (see Fig. 5a). The oxidation of adenine and guanine follows a two-step mechanism involving the total loss of $4e^-$, and the first $2e^-$ oxidation is rate-determining step. The slopes of 58 and 61 mV/pH shows that two protons take part in the rate-determining step [28]. The dependences of the oxidation peak currents of guanine and adenine on nano-copper oxide/GCE on pH are shown in Fig. 5b. The anodic peak currents improved with increasing solution pH and reached the maximum value when pH was equal to 7.0. The nano-copper oxide was alkaline-oxide, and its stability decreased with increasing solution acidity, resulting in the decrease of anodic peak. When pH of solution exceeded 7.0, the oxidation peak currents of guanine and adenine almost remained the same. Moreover, pH 7.0 was close to the physiological environment, and hence 0.1 M pH 7.0 PBS was chosen for the electrochemical detection of guanine and adenine.

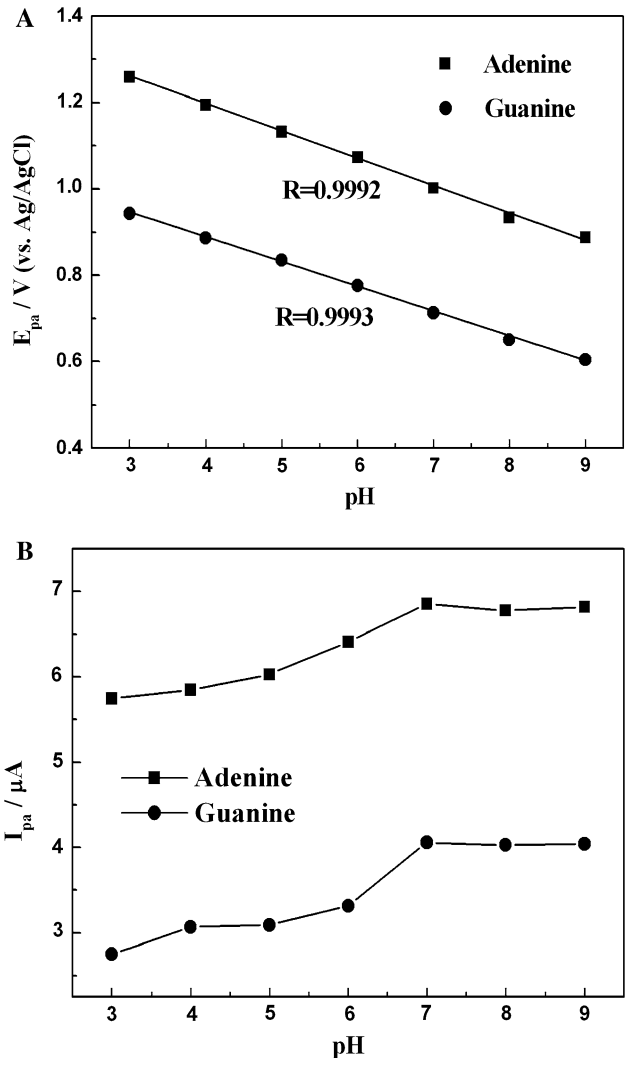

Fig. 5 **a** The relationship between the oxidation peak potentials of purine bases and solution pH on the nano-copper oxide/GCE. **b** The relationship between the oxidation peak currents of purine bases and solution pH on the nano-copper oxide/GCE

3.4 The anti-interference of nano-copper oxide/GCE sensor

In Fig. 6a, with the concentration of adenine being held at 0.5 μM, guanine was gradually added into the solution from 0 to 1.0 μM. It could be seen that the anodic peak current of guanine increased linearly with the anodic peak current of adenine being held at a constant value. In Fig. 6b, with the concentration of guanine being held at

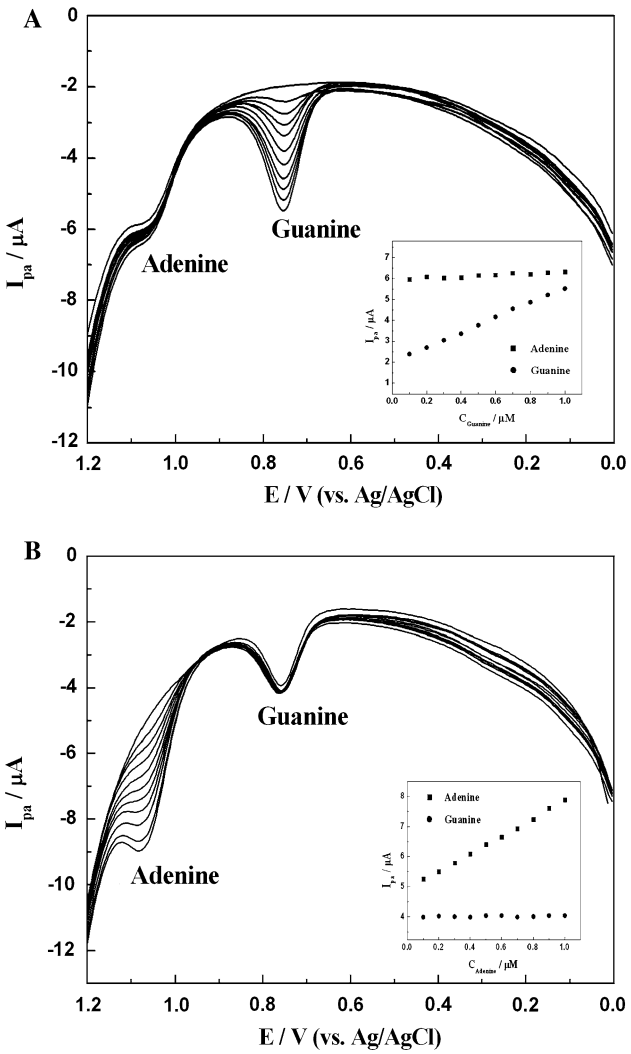

Fig. 6 **a** DPV curves for 0.5 μM adenine in the presence of 0, 0.1, 0.2, 0.3, 0.4, 0.5, 0.6, 0.7, 0.8, 0.9, and 1.0 μM guanine. **b** DPV curves for 0.5 μM guanine in the presence of 0, 0.1, 0.2, 0.3, 0.4, 0.5, 0.6, 0.7, 0.8, 0.9, and 1.0 μM adenine at the nano-copper oxide/GCE in 0.1 M PBS (pH 7.0). *Inset*: plot of anodic peak currents of adenine (guanine) versus the concentration of guanine (adenine)

0.5 μM, adenine was gradually added into the solution from 0 to 1.0 μM. The figure shows that the anodic peak current of adenine also increased linearly, when the anodic peak current of guanine was held at a constant value. These experiments illuminated that the presence of certain concentration of adenine (guanine) did not cause interference to guanine (adenine). Therefore, it is possible to determine quantitatively without any considerable influence on each other.

3.5 Simultaneous detection for guanine and adenine

Figure 7 shows the typical DPV curves of guanine and adenine using the nano-copper oxide/GCE with the increasing guanine and adenine concentrations. Linear relationship between peak current and purine bases concentration were attained over the range of 0.05–1.2 μM with the correlation coefficients of 0.9997 and 0.9993, respectively. The detection limits were estimated to be 6×10^{-3} μM and 9×10^{-3} μM for guanine and adenine, respectively (S/N = 3).

In order to explore the probability of the sensor application, the guanine and adenine in CT-DNA were detected by nano-copper oxide/GCE. Because the bases were embedded in the interior of the double helix, their detection was sterically hindered due to the crowed phosphate group on the exterior of the helix. Hence, the detection strategy of purine bases in nature DNA faced a poor sensitivity problem. The acid could digest DNA and make the double-strand completely unwinding. Therefore, all of the purine bases are exposed in the denatured DNA. In this study, the

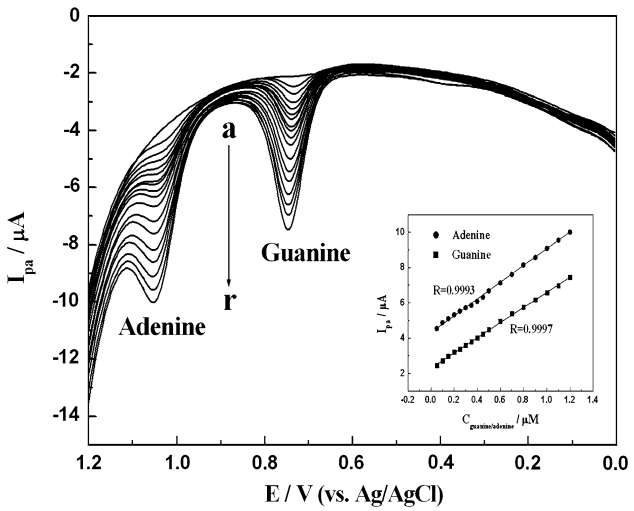

Fig. 7 DPV curves of 0, 0.05, 0.1, 0.15, 0.2, 0.25, 0.3, 0.35, 0.4, 0.45, 0.5, 0.6, 0.7, 0.8, 0.9, 1.0, 1.1, and 1.2 μM guanine and adenine on the nano-copper oxide/GCE in 0.1 M PBS (pH 7.0). *Inset*: Plot of anodic peak currents of adenine (guanine) versus the concentration of adenine (guanine)

Table 1 Contents of guanine and adenine in DNA simultaneously determined with nano-copper oxide/GCE ($n = 8$)

Calf thymus DNA treated by $HClO_4$	
Guanine (mol%)	22.37
Adenine (mol%)	27.63
Molar ratio ((G + C)/(A + T))	0.81

fabricated sensor was used to determine guanine and adenine in $HClO_4$ digested CT-DNA. When 10 μl denatured CT-DNA was added in a cell containing 5 ml 0.1 M pH 7.0 PBS, the oxidation peak currents of guanine and adenine were measured. Using the proposed method, the concentrations of guanine and adenine in DNA were obtained using a linear equation (see Table 1). The value (G + C)/(A + T) of 0.81 was attained for $HClO_4$-digested CT-DNA sample, and eight continuous measurements of 0.8 μg ml^{-1} CT-DNA showed good reproducibility with RSD = 3.1 %

4 Conclusions

The nano-copper oxide could be immobilized onto the surface of GCE by electrodeposition method to form a nano-copper oxide/GCE sensor. The nano-copper oxide film greatly facilitated the electron exchange between purine bases and electrode, improving the oxidation property of purine bases on electrode. The fabricated sensor was produced using simple preparation process, and it showed high sensitivity and low limit; so it could be used as an amperometric sensor for simultaneous detection of guanine and adenine.

References

1. McGown LB, Joseph M, Pitner J, Vonk G, Linn C (1995) Anal Chem 663A:67
2. Ribeiro ML, Priolli DG, Miranda DD, Arcari DP, Pedrazzoli J, Martinez CA (2008) Clin Colorectal Cancer 267:7
3. Kastan MB (2008) Mol Cancer Res 517:6
4. Mishra D, Pal S (2009) J Mol Str (Theochem) 96:902
5. Li SP, Li P, Dong TTX, Tsim KWK (2001) Electrophoresis 144:22
6. Malathi R, Johnson IM (2001) J Biomol Struct Dyn 709:18
7. Yang FQ, Guan J, Li SP (2007) Talanta 269:73
8. Wang HS, Ju HX, Chen HY (2002) Anal Chim Acta 243:461
9. Wang WP, Zhou L, Wang SM, Luo Z, Hu ZD (2008) Talanta 1050:74
10. Moral PG, Arin MJ, Resines JA, Diez MT (2005) J Chromatogr B 257:826
11. Klampfl CW, Himmelsbach M, Buchberger W, Klein H (2002) Anal Chim Acta 185:454
12. Xiong X, Jin OY, Baeyens WRG, Delanghe JR, Shen XM, Yang YP (2006) Electrophoresis 3243:27
13. Huang YC, Lin CC, Liu CY (2004) Electrophoresis 554:25

14. Wang P, Ren JC (2004) J Pharm Biomed Anal 277:34
15. Ganzera M, Vrabl P, Worle E, Burgstaller W, Stuppner H (2006) Anal Biochem 132:359
16. Liu EB, Xue BC (2006) J Pharm Biomed Anal 649:41
17. Heisler I, Keller J, Tauber R, Sutherland M, Fuchs H (2002) Anal Biochem 114:302
18. Amri CE, Baron MH, Maurel MC (2003) Spectrochim Acta, Part A 2645:59
19. Tang C, Yogeswaran U, Chen SM (2009) Anal Chim Acta 19:636
20. Sun W, Li YZ, Duan YY, Jiao K (2008) Biosens Bioelectron 988:24
21. Liu HY, Wang GF, Chen DL, Zhang W, Li CJ, Fang B (2008) Sens Actuat B-Chem 414:128
22. Patil SA, Patil LA, Patil DR, Jain GH, Wagh MS (2007) Sens Actuat B-Chem 246:123
23. Bennici S, Gervasini A, Ragaini V (2003) Ultrason Sonochem 61:10
24. Liu ZG, Zhou RX, Zheng XM (2007) J Mol Catal A-Chem 137:267
25. Le WZ, Liu YQ (2009) Sens Actuat B-Chem 147:141
26. Jia WZ, Guo M, Zheng Z et al (2008) Electroanalysis 2153:20
27. Reitz E, Jia WZ, Gentile M, Wang Y, Lei Y (2008) Electroanalysis 2482:20
28. Wang ZH, Xiao SF, Chen Y (2006) J Electroanal Chem 237:589